BMC Medical Imaging

RESEARCH

Open Access

Predictive value of high-risk esophageal varices in cirrhosis based on dual-energy CT combined with clinical and serologic features

Jiewen Chen[1†], Fei Zhang[1†], Shuitian Wu[1], Disi Liu[1], Liyang Yang[1], Meng Li[1], Ming Yin[1], Kun Ma[2], Ge Wen[1*] and Weikang Huang[1*]

Abstract

Objective To investigate the predictive value of dual-energy CT (DECT) in combination with clinical and serologic features for noninvasive assessment of high-risk esophageal variceal (EV) in cirrhosis patients.

Data and Methods 120 patients who had undergone DECT and gastroscopy were retrospectively enrolled. They were categorized into low-risk variceal (LRV) and high-risk variceal (HRV) groups by gastroscopy (LRV: none, mild, HRV: moderate, severe). Clinical data, serologic and DECT parameters were recorded respectively. Multifactorial logistic regression analyses were conducted to develop clinical, serological, DECT, and combined models. AUC was utilized to assess the diagnostic performance. Non-parametric tests were employed to analyze differences in DECT parameters among different grading of EV.

Results In clinical model, ascites was the independent risk predictor, with 78.3% accuracy,50% sensitivity, 100% specificity, and an AUC of 0.693. The serological model revealed white blood cell count, hematocrit, alanine aminotransferase, and platelet count as predictors for HRV, demonstrating 83.3% accuracy, 90.9% sensitivity, 76.9% specificity, and an AUC of 0.784. The DECT model, identified liver normalized iodine volume (NIV-L) and spleen volume (V-S) as key predictors, with 84% accuracy, 72.7% sensitivity, 92.9% specificity, and an AUC of 0.84. The combined model, integrating NIV-L, V-S, and Ascites, demonstrated superior performance with 82.6% accuracy, 90% sensitivity, 76.9% specificity, and an AUC of 0.878, compared to the other models. Additionally, severe EV had higher V-S and NIV-S values than other grades ($p < 0.05$), with AUC of 0.874 and 0.864, respectively.

Conclusion DECT-based NIV-L, V-S, and presence of ascites can predict high-risk esophageal varices.

Clinical relevance statement Quantitative parameters of DECT can predict high-risk esophageal varices in cirrhotic patients, avoid gastroscopy, if possible, continue hierarchical management.

†Jiewen Chen and Fei Zhang contributed equally to this work and should be considered as co-first authors..

*Correspondence:
Ge Wen
wenge@smu.edu.cn
Weikang Huang
3419216292@qq.com

Full list of author information is available at the end of the article

Trial registration retrospectively registered.

Key points

1. DECT quantitative parameters play an important role in predicting high-risk EV.
2. DECT combined with serology can better predict the occurrence of HRV.
3. This study avoids unnecessary endoscopy in a low-risk individuals.

Keywords Cirrhosis, Esophageal varices, Dual-energy CT, Normalized iodine volume, Spleen volume

Background

Esophageal gastric variceal bleeding (EGVB) is a common and severe complication occurring during the decompensated stage of portal hypertension in cirrhotic patients, marked by high mortality during acute episodes [1]. Approximately half of cirrhosis patients develop esophageal gastric varices, with 10–15% experiencing rupture and bleeding each year. In addition, nearly 12% of these patients develop portal hypertension, which is associated with a 20% mortality rate within six weeks of bleeding and a 60% risk of rebleeding within one year. These statistics highlight the substantial effect of EGVB on patient prognosis [2, 3]. Accurate prediction and stratification of high-risk patients for EGVB are essential for reducing hospitalization and mortality rates. Therefore, timely diagnosis and screening of cirrhotic patients at risk for EGVB is crucial.

Upper gastrointestinal endoscopy (UGE) is the cornerstone for diagnosing EGVB, providing detailed visualization of esophageal variceal morphology, size, and red signs. It is recommended by clinical guidelines for diagnosing esophageal gastric varices, screening patients, and assessing bleeding risk [4]. However, its invasive nature can hinder patient acceptance, lowering adherence to long-term follow-up examinations. Moreover, the procedure carries a risk of triggering EGVB and poses anesthesia-related risks for low-risk patients, complicating regular endoscopic monitoring. Measurement of the hepatic venous pressure gradient is the gold standard for diagnosing portal hypertension and evaluating treatment efficacy, as well as predicting the risk of variceal hemorrhage [2]. However, its invasiveness, requirement for specialized personnel and equipment, and high costs limit its widespread clinical use. Magnetic resonance elastography provides a noninvasive alternative for estimating EV [5], but it is affected by factors such as intrahepatic inflammation and iron deposition. Additionally, it presents challenges such as prolonged scan times, high costs, and the need for specialized equipment [6].

Recent high-quality studies have increasingly focused on the utility of CT imaging for evaluating esophageal varices and predicting bleeding events [7, 8]. Multi-slice spiral CT has proven effective in reliably detecting EVs and related hemorrhages, with the identification of collateral vessels—such as coronary, short gastric, and parietal esophageal branches—being significantly associated with these outcomes [9, 10]. Quantitative iodine concentration measurements in parenchymal organs, obtained through dual-energy CT (DECT) three-phase contrast-enhanced scans, reflect the degree of iodine uptake in liver and spleen tissues, which serves as an indicator of hepatic and splenic perfusion [11, 12]. Importantly, iodine concentration in the short gastric veins and spleen has been identified as an independent predictor of esophageal variceal bleeding (EVB) risk [13]. By integrating clinical features and CT radiomic characteristics of the liver and spleen, a predictive model has been developed, demonstrating superior accuracy in forecasting EGVB risk compared to existing noninvasive approaches [7]. These findings offered novel metrics for predicting bleeding risk and emphasized CT imaging's potential for precise EV assessment, which could enhance clinical decision-making. Therefore, incorporating CT imaging into the clinical management of EV, particularly for risk stratification and preventive strategies, is strongly recommended.

The limited literature on the association between quantitative iodine parameters from DECT scans of the liver and spleen and esophageal varices highlights the necessity for further research in this area [14]. Therefore, our study aimed to develop a noninvasive predictive model by combining DECT data, which captures quantitative hepatic and splenic perfusion metrics, with clinical serological markers. This integrated approach was designed to assess its prognostic efficacy in identifying high-risk esophageal varices in cirrhotic patients. Such a model could potentially reduce the need for endoscopic examinations in low-risk patients, improve patient stratification, and inform personalized treatment strategies.

Materials and methods

General information

A retrospective cohort of 120 cirrhotic patients was assembled, consisting of individuals admitted to our institution between March 2022 and January 2024, who underwent comprehensive diagnostic evaluations, including clinical history review, laboratory tests, and DECT. Each patient underwent both upper abdominal DECT enhancement scanning and gastrointestinal endoscopy, with a three-month interval between the two procedures. Notably, during the observation period,

none of the patients experienced EVB or received related therapeutic interventions. The study was approved by the hospital's ethics committee (NFEC-2024-378), allowing the informed consent to be waived due to the retrospective nature of the study.

The inclusion criteria were as follows: (1) Underwent an enhanced upper abdominal DECT scan (2). Had pathological or clinical evidence of cirrhosis (3). Completed serum marker analysis within 2 weeks of CT imaging and gastroscopy within 3 months.

The exclusion criteria were: (1) Patients who had received treatments for varices before admission, including endoscopic sleeve, tissue adhesive sclerotherapy, splenectomy, surgical shunts, partial splenic embolization, or transjugular intrahepatic portosystemic shunt (TIPS) (2). Patients with portal, splenic, or superior mesenteric vein thrombosis (3). Patients with a history of gastrointestinal hemorrhage within the past three months (4). Patients with a confirmed diagnosis of hepatocellular carcinoma based on histopathological findings. Flow chart of the study population see Fig. 1.

Examination methods

The GE Revolution Apex CT scanner was used to perform a series of scans, including plain, arterial, portal venous, and delayed phases. The scanning parameters included a pitch factor of 0.992:1, gantry rotation speed of 0.8 s/r, slice thickness of 5 mm, detector width of 80 mm, and a tube voltage of 140 kVp with instantaneous switching to 80 kVp (0.25 ms) during dual-energy CT, alongside automatic mA modulation. The scanning range covered from the diaphragm apex to the lower pole of the spleen. An enhanced scan was conducted with a nonionic iodine contrast agent (iophorol 350) at a dosage of 450 mgI/kg body weight, administered over 20 s, with the injection flow rate adjusted accordingly. The region of interest (ROI) for the arterial phase was set at the descending aorta, and scanning was triggered at 5.9 s when the threshold reached 150 HU. The portal venous phase scan was obtained 30 s after the arterial phase. The delay phase was obtained 100 s after the portal phase. All raw data were transferred to a GE AW 4.6 workstation, and DECT data were measured by two physicians with

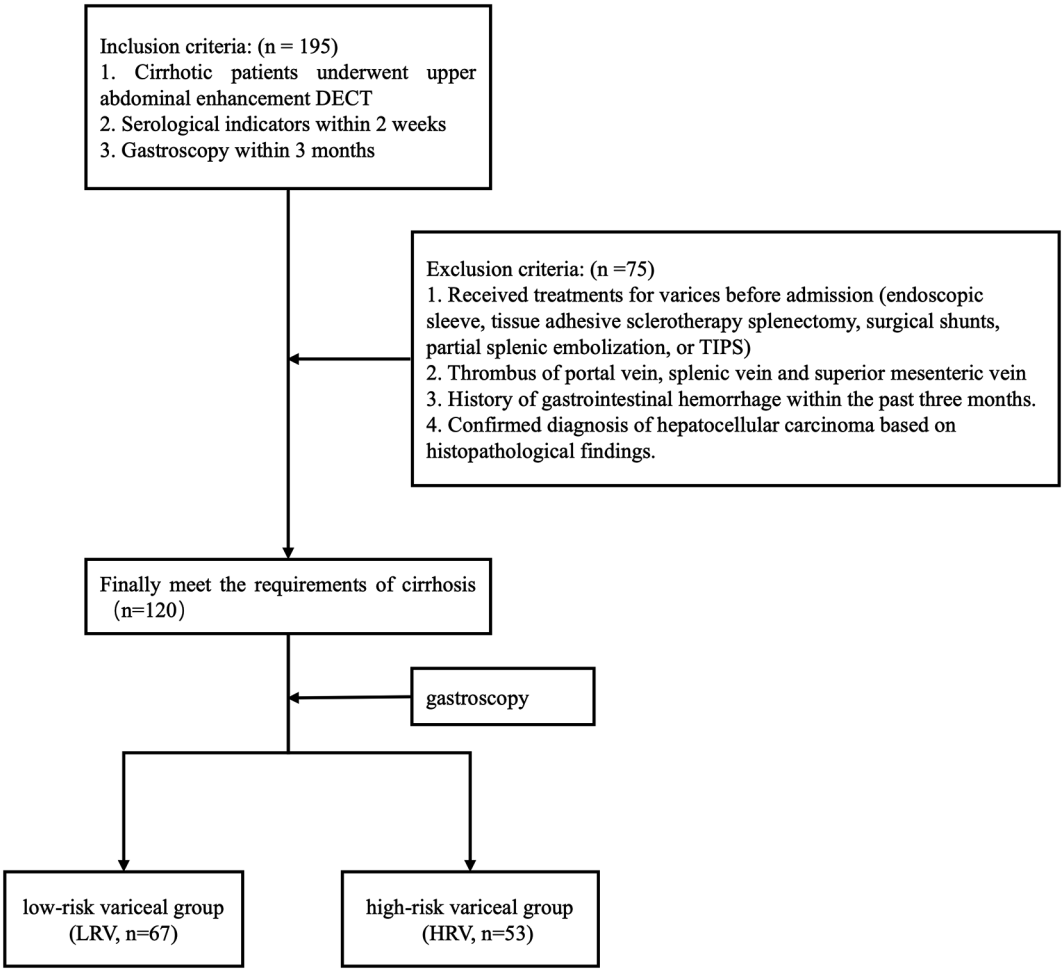

Fig. 1 Flow chart of the study population

over 5 and 10 years of experience in diagnostic abdominal imaging, respectively.

Patients were classified into four categories based on the severity of EV observed during endoscopy: no EV (EV0), mild EV (EV1), moderate EV (EV2), and severe EV (EV3). The classification criteria were as follows [15–17]: mild EV was characterized by varices with a linear or slightly tortuous morphology without red signs; moderate EV included varices that were linear or slightly tortuous with red signs, or that exhibited a serpentine appearance without red signs; and severe EV was defined by a serpentine configuration with red signs, or by a beaded, nodular, or neoplastic appearance, with or without red signs. All assessments were performed by a gastroenterologist with over 10 years of experience in diagnostic gastrointestinal endoscopy. Based on the likelihood of developing EVB, patients were further categorized into a high-risk variceal group (HRV) comprising those with EV2 and EV3, and a low-risk variceal group (LRV) including those with EV0 and EV1.

Post-processing of DECT images

The Volume Viewer software on the GE AW 4.6 workstation was used to automatically calculate the liver and spleen volumes. This was achieved by manually outlining the organ contours layer by layer from the top to the lower edge in the portal phase images while avoiding large vessels. Surrounding fat and vascular structures were excluded by adjusting the threshold range.

Iodine-water material images of the liver and spleen were obtained using the AW 4.6 workstation. Five 200 mm^2 regions of interest were defined at the hepatic hilar plane, where the right and left portal vein branches converge, carefully excluding vasculature and bile ducts. Iodine concentration measurements were taken in different liver lobes (left outer, left inner, right anterior, right posterior, and caudate lobes) and the abdominal aorta. All values were measured by two senior radiologists and averaged. The mean iodine concentration in the liver (MIC-L) was calculated as the average of these five ROI values and expressed in units of 100 μg/cm^3. Additionally, the liver normalized iodine concentration (NIC-L) was calculated as MIC-L divided by the iodine concentration in the abdominal aorta (IC_{aor}).

Circular ROIs, each with an area of approximately 200 mm^2, were positioned in the upper, middle, and lower segments of the spleen, carefully excluding vascular structures. The spleen mean iodine concentration (MIC-S) was calculated as the average iodine concentration across these three ROIs. The spleen normalized iodine concentration (NIC-S) was calculated as MIC-S divided by the IC_{aor}. To account for variations in blood circulation rates, the iodine concentration ratios were normalized. The normalized iodine volume for the liver (NIV-L) and spleen (NIV-S) was calculated using the formula NIV = V × NIC, where V represents the volume of the liver or spleen. See Fig. 2.

Statistical methods

Statistical analyses were performed using SPSS version 25.0 and R Programming Language. The normality of the measurement data was assessed using the Kolmogorov-Smirnov test. For normally distributed data, descriptive statistics were reported as mean ± standard deviation ($x \pm s$), with inter-group comparisons conducted via independent samples t-tests. Non-normal distributions were characterized by Median (IQR), and corresponding group comparisons were performed using Mann-Whitney U tests. Categorical variables were summarized through frequency counts and analyzed using χ^2 contingency table tests.

Univariate and multivariate binary logistic regression analyses were performed. Variables found to be statistically significant in the univariate analysis were included in the multivariate regression. Based on this, four logistic regression models were developed: a clinical model, a serological model, a DECT-based model, and a combined model. The combined model was constructed by incorporating all variables identified as significant through multivariate logistic regression analysis. To evaluate model performance, five-fold cross-validation was applied to each of the four models. Diagnostic effectiveness in identifying high-risk EVs was assessed by plotting receiver operating characteristic (ROC) curves, calculating the area under the curve (AUC), and evaluating model calibration using calibration curves. Differences in AUC values were compared using the DeLong test.

Non-parametric tests were employed to assess differences in liver and spleen DECT measurements across the four endoscopic groups. The Kruskal-Wallis test was used for pairwise comparisons within these groups. ROC curves were plotted to determine AUC values for the diagnostic performance of each group in detecting severe EV. A p-value of less than 0.05 was considered statistically significant for all analyses.

Results

Comparison of clinical, serological, and DECT features between the HRV and LRV

A cohort of 120 patients, including 98 males and 22 females, was enrolled in the study. Liver function was assessed using the Child-Pugh classification, with 76 patients graded as A, 31 as B, and 13 as C. Sixty-seven patients were classified into the low-risk group, while 53 were categorized into the high-risk group. The clinical parameters examined included age, Child-Pugh class, and the presence of ascites, along with various hematologic indices (WBC, RBC, HGB, HCT, PLT, and FIB-4),

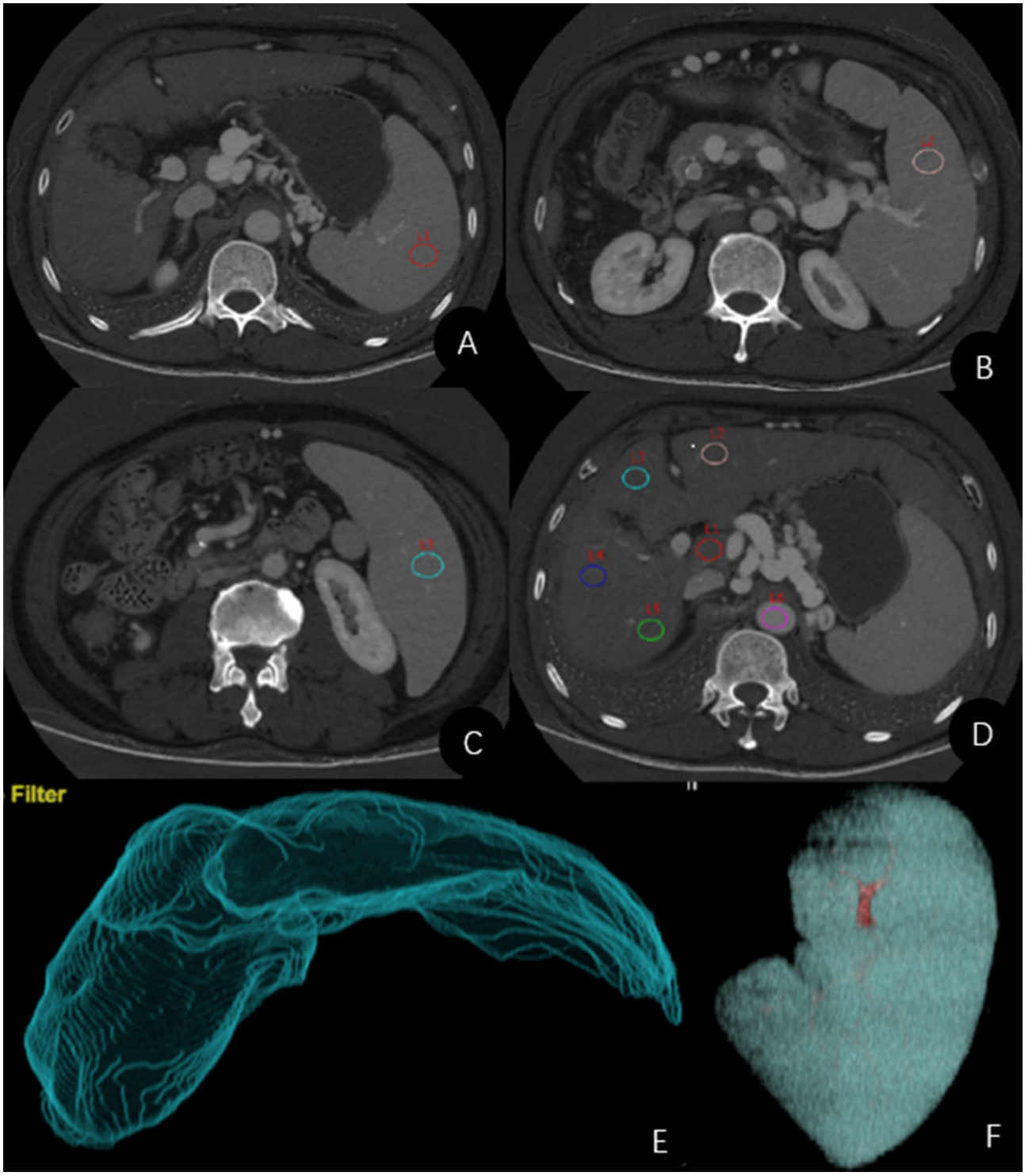

Fig. 2 Measurement of DECT parameters. **A**-**C** Splenic iodine concentration measured in the upper, middle, and lower portions of the spleen during the portal venous phase; **D** Hepatic parenchymal iodine concentration; **E** Liver volume measurements; **F** Splenic volume measurements

and DECT parameters (including NIV and volume of the liver and spleen, and liver NIC), all of which showed statistical significance ($p < 0.05$). The liver volume, NIC, and NIV were significantly associated with esophageal varices progression ($p < 0.05$). As esophageal varices worsened, liver volume and NIV increased, whereas spleen volume and NIV decreased, as detailed in Table 1.

Construction and evaluation of risk prediction models for HRV and LRV groups

Clinical model

In univariate logistic regression analysis, age, ascites, and Child-Pugh class were identified as risk factors for developing HRV. These variables were incorporated into a binary logistic regression model, which identified the presence of ascites as an independent risk predictor for high-risk esophageal varices. Patients with ascites had an 8.25-fold higher risk of developing high-risk EV compared to those without ascites, as shown in Table 2.

Serological model

Univariate logistic regression analysis of the serological indicators showed that all parameters, except HGB and AST, were significant risk factors for HRV. The significant parameters were then included in a binary logistic regression model, which identified WBC, HCT, AST and PLT as independent risk predictors for high-risk EV, with odds ratios (OR) of 0.77, 0.00, 0.98and 0.99, respectively, as demonstrated in Table 2.

DECT model

Univariate logistic regression analysis showed that all DECT parameters, except NIC-S, were significant risk factors. The parameters with significant associations were then incorporated into a binary logistic regression model. The results indicated the decreased NIV-L and increased V-S were associated with high-risk EV, with OR of 1.00 and 1.00, respectively, as shown in Table 2.

Combined model

The independent risk factors (Ascites, WBC, HCT, AST, PLT, V-S, and NIV-L) in the above three models were used to construct a new binary Logistic regression model. The results showed that NIV-L, V-S, and Ascites were independent risk predictors for high-risk EV. OR values were 1.00, 1.00, and 8.11, respectively. For each unit increase in NIV-L and V-S, the risk of developing high-risk esophageal varices was 1 time. Patients with ascites were 8.11 times more likely to have high-risk esophageal varices than patients without ascites, as illustrated in Table 2.

Table 1 Comparison of clinical, serological and DECT features between LRV and HRV

Parameter			LRV($n=67$)	HRV($n=53$)	Test(t/χ^2 / z)	*P*-Value
Clinical	Age (years)		49.64 ± 11.50	54.25 ± 11.05	2.215	0.029
	Gender, Male(%)	Man	54(80.6%)	44(83.0%)	0.116	0.733
	Etiology of cirrhosis	Hepatitis	48(71.6%)	38(71.7%)	0.397	0.82
		Alcohol abuse	12(17.9%)	11(20.7%)		
		Miscellaneous	7(10.4%)	4(7.5%)		
	Child-Pugh class	A	52(77.6%)	24(45.3%)	13.461	0.001
		B	10(14.9%)	21(39.6%)		
		C	5(7.5%)	8(15.1%)		
	Ascites	No	60(89.6%)	27(50.9%)	22.124	<0.001
		Yes	7(10.4%)	26(49.1%)		
Laboratory	WBC(/L)		5.55(2.37)	3.65(2.43)	-4.146	<0.001
	RBC(10^9/L)		4.25(1.31)	3.69(1.48)	-2.814	0.005
	HGB(g/L)		132(37)	114(53)	-3.42	<0.001
	HCT(%)		0.39(0.09)	0.33(0.14)	-3.832	<0.001
	PLT(10^9/L)		118(79)	64(43)	-4.796	<0.001
	ALB(g/L)		38.98(8.73)	33.65(11.73)	-2.944	0.003
	TP(g/L)		69.78 ± 7.59	66.74 ± 8.15	2.106	0.037
	AST(U/L)		44.74(54.58)	42.44(29.97)	-1.165	0.244
	ALT(U/L)		42(80.23)	28.92(26)	-2.782	0.005
	AST/ALT		1.05(0.83)	1.3(0.86)	-2.465	0.014
DECT	V-L(cm^3)		1215(445)	1037(443)	-2.531	0.011
	V-S(cm^3)		313.11(204.19)	629.87(510.45)	-5.811	<0.001
	NIC-L		0.538 ± 0.10	0.492 ± 0.08	2.816	0.006
	NIC-S		0.625(0.068)	0.622(0.102)	-0.449	0.653
	NIV-L		638.89(380.41)	509.51(233.58)	-3.247	0.001
	NIV-S		191.15(145.50)	391.51(310.08)	-5.663	<0.001

Table 2 Univariate and multivariable logistic regression analysis associated with the four models of LRV and HRV

		Univariate logistic regression analysis		Multivariable logistic regression analysis	
	Variable	**OR**	**P**	**OR (95%CI)**	**P**
Clinical model	Age (years)	1.037	0.032		
	Gender	/	/		
	Etiology of cirrhosis	/	/		
	Ascites	8.254	<0.001	8.25(3.34,22.81)	<0.001
	Child-pugh class		0.002		
	Child-pugh class (1)	4.550	0.001		
	Child-pugh class (2)	3.467	0.045		
	Constant			/	<0.001
Serological model	**WBC**	0.640	<0.001	0.77(0.60,0.98)	0.040
	RBC	0.624	0.011		
	HGB	/	/		
	HCT	0.000	<0.001	0.00(0.00,0.52)	0.031
	PLT	0.982	<0.001	0.99(0.98,1.00)	0.035
	ALB	0.930	0.009		
	TP	0.952	0.041		
	AST	/	/		
	ALT	0.984	0.004	0.98(0.97,0.99)	0.011
	AST/ALT	1.760	0.041		
	Constant			/	<0.001
DECT model	V-L	0.999	0.022		
	V-S	1.004	<0.001	1.00(1.00,1.01)	<0.001
	NIC-L	0.002	0.008		
	NIC-S	/	/		
	NIV-L	0.997	0.003	1.00(0.99,1.00)	0.003
	NIV-S	1.007	<0.001		
	Constant			/	0.442
Combined model	NIV-L			1.00(0.99,1.00)	0.007
	V-S			1.00(1.00,1.01)	<0.001
	Ascites			8.11(2.70,27.74)	<0.001
	Constant			/	0.162

Table 3 Comparison of four models

Models	Variables	AUC	95% CI	Cutoff value	Sensitivity	Specificity	PPV	NPV	Accuracy
Clinical model	Ascites	0.693	0.648,0.749	0.534	50.0%	100.0%	100.0%	72.2%	78.3%
Serological model	PLT, ALT, HCT, WBC	0.784	0.681,0.864	0.313	90.9%	76.9%	76.9%	90.9%	83.3%
DECT model	V.S, NIV.L	0.84	0.709,0.952	0.448	72.7%	92.9%	88.9%	81.3%	84.0%
Combined model	V.S, Ascites, NIV.L	0.878	0.778,0.976	0.317	90.0%	76.9%	75.0%	90.9%	82.6%

Evaluation of the predictive performance of four models

The AUC for the clinical, serological, DECT, and combined models was 0.693, 0.784, 0.84, and 0.878, respectively. When the Youden index is at its maximum, the optimal cut-off value of the combined model is 0.317, with a sensitivity of 90% and a specificity of 76.9%. Compared with other models, this model has better diagnostic efficacy and higher authenticity. DeLong test showed that the combined model had statistically significant differences with clinical and serological models ($P \le 0.01$), but no significant differences with DECT model. The calibration curve demonstrates that the combined model's predicted probabilities closely align with the diagonal of the calibration plot, indicating reliable calibration of the model.These results are shown in Table 3; Fig. 3.

Comparison between gastroscopy four groups of liver and spleen DECT parameters and ROC curve analysis

Nonparametric tests indicated statistically significant overall differences in liver and spleen volume, as well as NIV, across the four groups (EV0-EV3) ($p < 0.05$), as shown in Table 4. Patients with more severe EV demonstrated higher V-S and NIV-S, as illustrated in Fig. 4. In pairwise comparisons, significant differences in V-S and NIV-S were observed between patients with EV3 and those with lower grades (EV0, EV1, EV2) ($p < 0.05$),

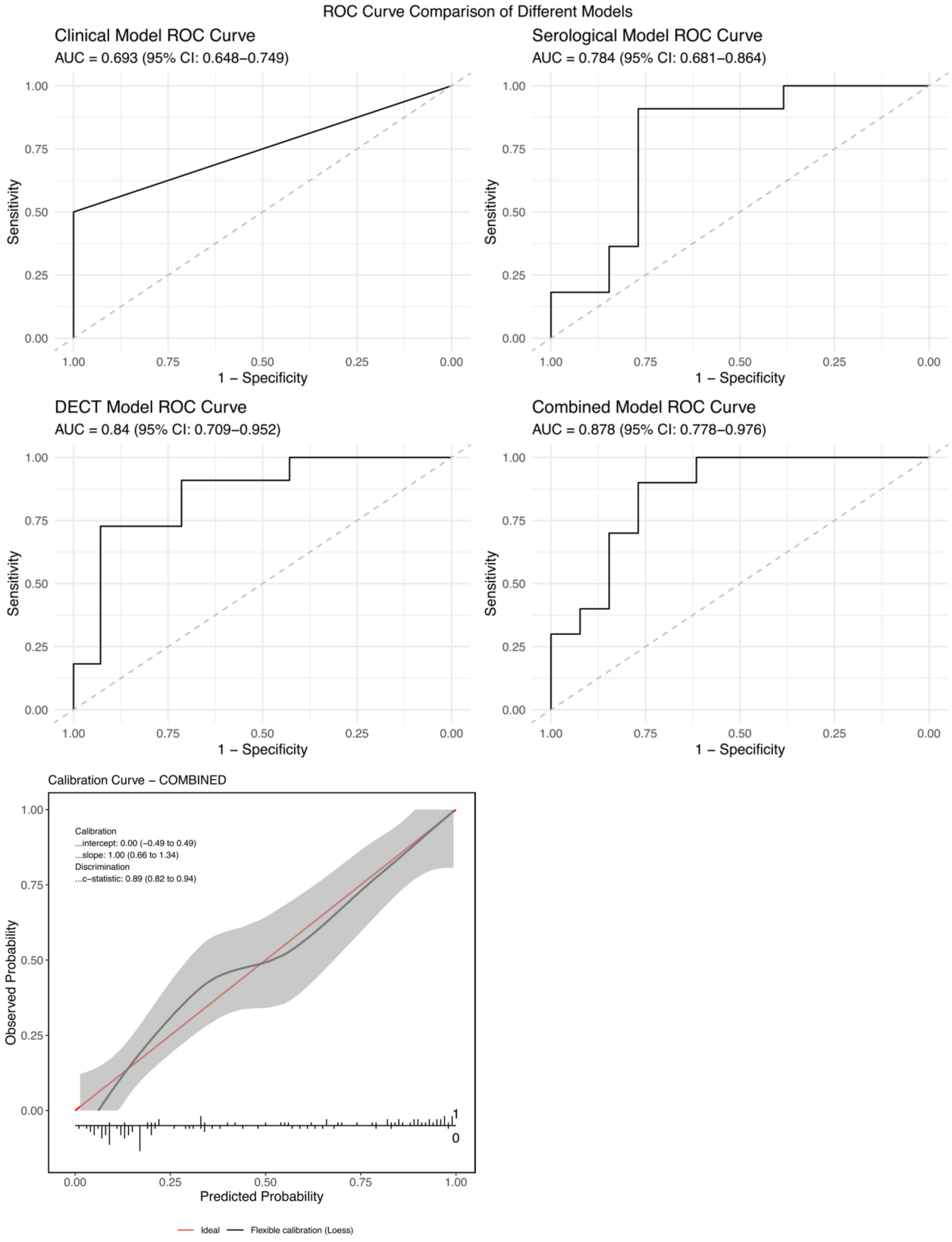

Fig. 3 ROC curve for predicting HRV and calibration curve of combined model

Table 4 Comparison of DECT features between four groups

Groups	Number	V-L	V-S	NIV-L	NIV-S
EV0	50	1299(456)	307.59(216.95)	680.06(343.82)	190.20(157.49)
EV1	17	1009(657)	342.84 (353.28)	513.35(394.95)	214.94(290.82)
EV2	16	1194(399)	367.44(475.77)	579.93(269.08)	245.03(264)
EV3	37	955(365)	792.54(565.18)	495.10(258.60)	442.94(305.13)
Z		14.663	45.394	19.279	42.861
P		**0.002**	**<0.001**	**<0.001**	**<0.001**

Note. V-L, liver volume; V-S, splenic volume; N IV-L, normalized iodine capacity in liver; N IV-S, normalized iodine capacity in splenic

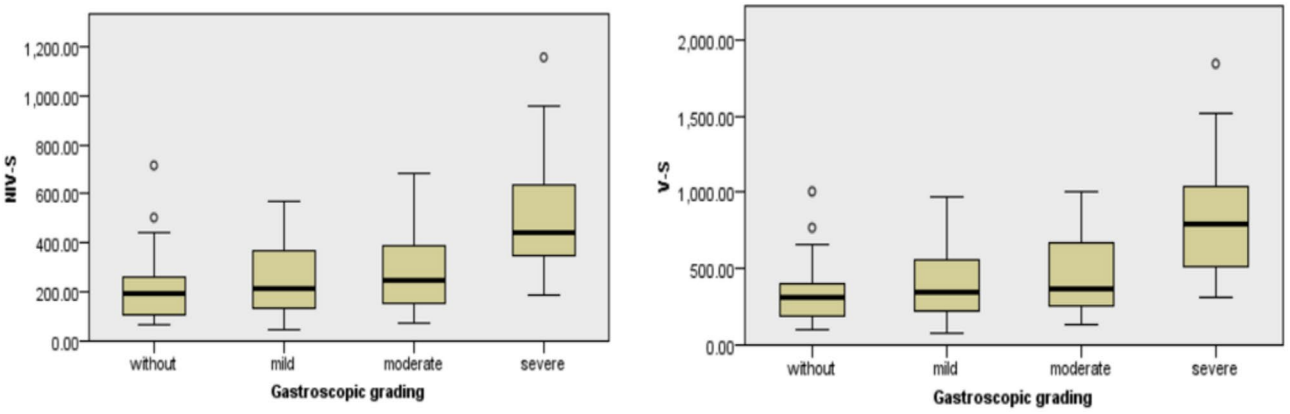

Fig. 4 Boxplot of gastroscopic grades in NIV-S, V-S

Table 5 Pairwise comparison of V-S, IV-S between four groups

Comparison	V-S (Median [IQR])	*p*-value	NIV-S (Median [IQR])	*p*-value
V3 vs. V0	792.54(565.18) vs. 307.59(216.95)	< 0.001	442.94(305.13) vs. 190.20(157.49)	< 0.001
V3 vs. V1	792.54(565.18) vs. 342.84 (353.28)	< 0.001	442.94(305.13) vs. 214.94(290.82)	< 0.001
V3 vs. V2	792.54(565.18) vs. 367.44(475.77)	0.006	442.94(305.13) vs. 245.03(264)	0.009

as shown in Table 5. The ROC curve analysis for V-S and NIV-S in predicting the severity of EV is presented in Fig. 5, with AUC values of 0.874 and 0.864, respectively.

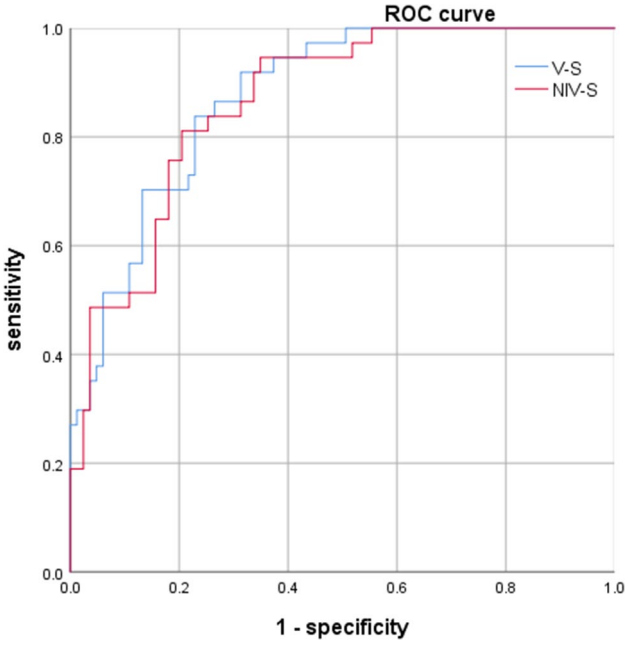

Fig. 5 ROC curve of V-S and NIV-S for predicting EV degree

Discussion

Bleeding from esophagogastric fundic varices is a serious complication of cirrhosis or portal hypertension, with consistently high incidence rates. Our study developed a predictive model for identifying HRV by integrating hepatic and splenic hemodynamic parameters from DECT with clinical and serological characteristics. The results indicated that NIV-L, V-S, and the presence of ascites are strong predictors of HRV. Moreover, the combined model showed a higher AUC compared to the individual clinical, serological, and DECT models. The DeLong test confirmed a significant difference between the combined model and the clinical, serological models. Notably, V-S and NIV-S were useful in further distinguishing severe varices (EV3), with higher values observed in patients with more advanced varices.

The Baveno VI guidelines suggest that endoscopic screening may be avoided in patients with compensated advanced chronic liver disease who have liver

stiffness < 20 kPa and a platelet count (PLT) > 150,000/μL [16]. This highlights the diagnostic value of PLT as a routine parameter in identifying esophageal varices in multimetric diagnostic models [18]. In our study, PLT was identified as an independent predictor for HRV within the serological model, consistent with previous research. Ascites, a common manifestation of decompensated cirrhosis, results from a combination of portal hypertension and hepatic dysfunction. Patients with hepatitis C cirrhosis and esophageal varices often exhibit more severe ascites, indicating its critical role in variceal formation [19]. Moreover, a significant association between portal hypertensive gastropathy and ascites has been demonstrated, with ascites severity correlating positively with the extent of portal hypertension [20]. Our findings showed that cirrhotic patients with ascites are at significantly increased risk of developing HRV, with odds ratios of 8.25 and 8.11 in the clinical and combined models, respectively, compared to those without ascites, underscoring the importance of ascites.

DECT offers non-invasive imaging with high reproducibility, superior image resolution, and a lower radiation dose compared to CT perfusion techniques [21]. The core principle of substance decomposition in DECT relies on the distinct X-ray absorption patterns of specific substances, enabling their isolation for quantitative analysis through material differentiation. The iodine concentration displayed in the iodine base map of DECT directly reflects the iodine uptake of tissues and organs, serving as an indirect indicator of their blood supply [22]. Previous studies have shown a strong correlation between iodine concentrations in the liver and spleen and CT perfusion indexes in characterizing hemodynamic changes [23]. The NIV, calculated as the product of organ volumes and their respective normalized iodine concentrations, offers a quantitative assessment of the overall blood flow dynamics in the liver and spleen.

It has been found that a radiological model based on contrast-enhanced CT images can accurately diagnose clinically significant liver fibrosis [24, 25]. This suggests that CT enhanced images contain a huge amount of information in the aspect of severe fibrosis and cirrhosis of the liver, which can be further explored. We observed a strong correlation between liver volume, NIV, and the severity of EV, with significant differences observed across the EV0-EV3 groups. NIV reflected hepatic perfusion during the portal venous phase.In cirrhosis, portal venous flow is obstructed due to liver fibrosis and structural alterations in hepatic sinusoids, leading to increased intravascular hydrostatic pressure in the portal vein and its branches, which results in the formation of collateral circulation [9, 26]. Previous research has shown that CT-derived quantitative parameters, such as hepatic lobe volume and the presence of ascites, can effectively predict severe varices within diagnostic models [27]. Fu et al. demonstrated that the standardized iodine concentration in the hepatic parenchyma during the portal phase significantly affects the risk of esophageal variceal rupture and bleeding, achieving an AUC of 0.860 in their model incorporating clinical factors [28]. Another study found that liver NIC performed well in identifying clinically significant portal hypertension (≥ 10 mmHg), esophageal varices, and high-risk varices, with AUC values of 0.951, 0.932, and 0.960, respectively, further supporting its utility in assessing portal pressure in cirrhotic patients [29]. These findings, together with our results, demonstrated a clear relationship between liver volume, iodine concentration, and the severity of esophageal varices, confirming that hepatic NIV is an independent predictor of high- and low-risk varices and is reflective of EV severity.

This study identified a significant correlation between spleen volume and NIV with the severity of EV. We found that each unit increase in spleen volume was associated with a 1-fold increase in the risk of HRV. Comparative analysis across the EV0 to EV3 patient groups revealed substantial differences in spleen volume and NIV, with individuals who had advanced EV showing elevated values, indicating increased splenic blood volume in cirrhosis complicated by portal hypertension. This phenomenon may result from obstruction of splenic vein branches due to portal hypertension, which triggers increased splenic lymphatic activity and angiogenesis. These changes lead to congestive splenomegaly and hypersplenism, altering splenic hemodynamics and playing a crucial role in the progression of portal hypertension and variceal formation [30]. Supporting evidence from Lee et al. demonstrated that the splenic volume-to-platelet ratio, derived using CT deep learning, effectively identified high-risk varices and predicted bleeding risk [31]. Similarly, Tani et al. found that splenic extracellular volume and volumetric data from routine CT scans predicted high-risk esophagogastric varices with 87% accuracy [32]. These findings highlighted spleen volume as an independent predictor of HRV.

In this study, the diagnostic performance of spleen volume and NIV for determining the severity of EV, as assessed by gastroscopy, was strong, with AUC values of 0.874 and 0.864, respectively. These findings suggested that these parameters could be valuable for stratifying esophageal varices severity in cirrhotic patients. Additionally, Liu et al. identified splenic iodine concentration as an independent predictor of EVB [13], while Han et al. reported significantly elevated splenic iodine volumes in cirrhotic patients compared to those with normal liver function [14]. Although splenic iodine quantification has proven critical in predicting HRV, splenic NIV was excluded from the DECT model used for HRV

identification, and the rationale for this exclusion remains unclear and warrants further investigation.

This study integrated DECT with clinical and serological indices to examine liver and spleen morphology and function. However, several limitations must be acknowledged. First, the retrospective design, small sample size, uneven patient distribution, and potential selection bias emphasize the need for a larger, more balanced cohort, especially with greater representation of mild and moderate EV, to more robustly validate these findings. Second, as a single-centre study conducted in a specific hospital, the generalisability and reproducibility of the results may be limited, and the model needs to be externally validated in a multicentre cohort. Future studies could further refine the model to make it more useful in clinical practice. Third, while DECT iodine concentration provides a static assessment of iodine distribution, using more precise blood perfusion techniques, such as CT perfusion, could improve accuracy. Finally, the potential of ultrasound transient elastography for predicting portal hypertension and esophageal varices should be compared with the DECT model to more comprehensively evaluate diagnostic performance.

In conclusion, integrating DECT with clinical and serological assessments demonstrated strong predictive ability for identifying high-risk varices (HRV) in cirrhotic patients. DECT measurements, including the NIV of the liver and spleen, as well as spleen volume, provide critical insights for assessing and predicting HRV. This comprehensive approach enhanced patient stratification and supports targeted therapeutic interventions to prevent clinical decompensation, while reducing the need for unnecessary procedures, such as upper gastrointestinal endoscopy (UGE), in low-risk patients.

Abbreviations

DECT	Dual energy computed tomography
EGVB	Esophageal gastric variceal bleeding
ROI	Region of interest
AUC	Area under the receiver operating characteristic curve
EV	Esophageal varices
HRV	High-risk variceal
LRV	Low-risk variceal
V-S, V-L	Volume of liver or spleen
NIV-L, NIV-S	Ormalized iodine volume in the liver or spleen

Author contributions

WH and GW conceived the study. JC and FZ designed the study, LY, MY and ML collated the data, KM and JC carried out data analyses and produced the initial draft of the manuscript. JC, FZ, SW, DL contributed to drafting the manuscript. All authors have read and approved the final submitted manuscript.

Funding

The authors state that this work has not received any funding.

Data availability

The data that support the findings of this study are available from the corresponding author upon reasonable request.

Declarations

Ethics approval and consent to participate

The retrospective study was conducted in accordance with the Declaration of Helsinki (as revised in 2013). The content of the study was eligible for an ethics exemption.

Human ethics and consent to participate

Not applicable.

Consent for publication

Oral informed consent has been obtained from the patients to publish their anonymous information in this article.

Competing interests

The authors declare no competing interests.

Author details

[1]Department of Radiology, Nanfang Hospital Zengcheng Campus, Southern Medical University, Guangzhou 511338, China
[2]CT Imaging Research Center, GE HealthCare China, Tianhe District, Huacheng Road 87, Guangzhou 510623, China

Received: 17 November 2024 / Accepted: 18 April 2025
Published online: 25 April 2025

References

1. Lesmana C, Raharjo M, Gani RA. Managing liver cirrhotic complications: overview of esophageal and gastric varices. Clin Mol Hepatol. Oct. 1 2020;26(4):444–60.
2. de Franchis R, Bosch J, Garcia-Tsao G, Reiberger T, Ripoll C. Baveno VII - Renewing consensus in portal hypertension. J Hepatol. Apr. 1 2022;76(4):959–74.
3. Jakab SS, Garcia-Tsao G. Evaluation and management of esophageal and gastric varices in patients with cirrhosis. Clin Liver Dis. Aug. 1 2020;24(3):335–50.
4. Garcia-Tsao G, Abraldes JG, Berzigotti A, Bosch J. Portal hypertensive bleeding in cirrhosis: risk stratification, diagnosis, and management: 2016 practice guidance by the American association for the study of liver diseases. Hepatology. Jan. 1 2017;65(1):310–35.
5. Abe H, Midorikawa Y, Matsumoto N, Moriyama M, Shibutani K, Okada M et al. Prediction of esophageal varices by liver and spleen MR elastography. Eur Radiol. Dec. 1 2019;29(12):6611–9.
6. Stankovic Z. Four-dimensional flow magnetic resonance imaging in cirrhosis. World J Gastroentero. Jan. 7 2016;22(1):89–102.
7. Luo R, Gao J, Gan W, Xie WB. Clinical-radiomics nomogram for predicting esophagogastric variceal bleeding risk noninvasively in patients with cirrhosis. World J Gastroentero. Feb. 14 2023;29(6):1076–89.
8. Gao Y, Yu Q, Li X, Xia C, Zhou J, Xia T et al. An imaging-based machine learning model outperforms clinical risk scores for prognosis of cirrhotic variceal bleeding. Eur Radiol. Dec. 1 2023;33(12):8965–73.
9. Wan S, He Y, Zhang X, Wei Y, Song B. Quantitative measurements of esophageal varices using computed tomography for prediction of severe varices and the risk of bleeding: a preliminary study. Insights Imaging. March 14 2022;13(1):47.
10. Ryu H, Kim TU, Yoon KT, Hong YM. Predicting the risk of early bleeding following endoscopic variceal ligation in cirrhotic patients with computed tomography. BMC Gastroenterol. Nov. 24 2023;23(1):410.
11. Shang S, Cao Q, Han X, Wang Y, Yin C, Zhao L. Assessing liver hemodynamics in children with cholestatic cirrhosis by use of Dual-Energy spectral CT. Am J Roentgenol. March 1 2020;214(3):665–70.
12. Bak S, Kim JE, Bae K, Cho JM, Choi HC, Park MJ et al. Quantification of liver extracellular volume using dual-energy CT: utility for prediction of liver-related events in cirrhosis. Eur Radiol. Oct. 1 2020;30(10):5317–26.
13. Liu H, Sun J, Liu X, Liu G, Zhou Q, Deng J et al. Dual-energy computed tomography for non-invasive prediction of the risk of oesophageal variceal bleeding with hepatitis B cirrhosis. Abdom Radiol. Nov. 1 2021;46(11):5190–200.
14. Han X, An W, Cao Q, Liu C, Shang S, Zhao L. Noninvasive evaluation of esophageal varices in cirrhotic patients based on spleen hemodynamics: a dual-energy CT study. Eur Radiol. June 1 2020;30(6):3210–6.

15. [Guidelines on the management. Of esophagogastric variceal bleeding in cirrhotic portal hypertension]. Zhonghua Nei Ke Za Zhi. Jan. 1 2023;62(1):7–22.
16. de Franchis R. Expanding consensus in portal hypertension: report of the Baveno VI consensus workshop: stratifying risk and individualizing care for portal hypertension. J Hepatol. Sep. 1 2015;63(3):743–52.
17. Hong S, Kim JE, Cho JM, Choi HC, Won JH, Na JB et al. Quantification of liver extracellular volume using dual-energy CT for ruling out high-risk varices in cirrhosis. EUR J RADIOL [Journal Article]. 2022 2022-3-1;148:110151.
18. Yan Y, Xing X, Wang X, Men R, Luo X, Yang L. Development and validation of an Easy-to-Use risk scoring system for screening High-Risk varices in patients with HBV-Related compensated advanced chronic liver disease. DIGEST DIS SCI. [Journal Article; Research Support, Non-U.S. Gov't; Validation Study]. 2021 2021-12-1;66(12):4518–24.
19. Ali SM, Farrukh S, Haqqi S, Siddiqui AR, Qadri MZ, Niaz SK. Oesophageal varices and associated factors in cirrhotic patients with hepatitis C. J Ayub med coll Abbottabad. [Journal Article]. 2022 2022-10-1;34(4):834–7.
20. Wu R, Liu K, Shi C, Tian H, Wang N. Risk factors for portal hypertensive gastropathy. BMC GASTROENTEROL [Journal Article]. 2022 2022-10-14;22(1):436.
21. Mule S, Pigneur F, Quelever R, Tenenhaus A, Baranes L, Richard P et al. Can dual-energy CT replace perfusion CT for the functional evaluation of advanced hepatocellular carcinoma? EUR RADIOL. [Journal Article]. 2018 2018-5-1;28(5):1977–85.
22. Dong J, He F, Wang L, Yue Z, Wen T, Wang R et al. Iodine density changes in hepatic and Splenic parenchyma in liver cirrhosis with dual energy CT (DECT): A preliminary study. ACAD RADIOL. [Journal Article]. 2019 2019-7-1;26(7):872–7.
23. Lv P, Lin X, Gao J, Chen K. Spectral CT: preliminary studies in the liver cirrhosis. KOREAN J RADIOL [Journal Article]. 2012 2012-7-1;13(4):434–42.
24. Tang M, Wu Y, Hu N, Lin C, He J, Xia X et al. A combination model of CT-based radiomics and clinical biomarkers for staging liver fibrosis in the patients with chronic liver disease. SCI REP-UK. [Journal Article]. 2024 2024-8-30;14(1):20230.
25. Wang J, Tang S, Mao Y, Wu J, Xu S, Yue Q et al. Radiomics analysis of contrast-enhanced CT for staging liver fibrosis: an update for image biomarker. HEPATOL INT. [Journal Article; Randomized Controlled Trial]. 2022 2022-6-1;16(3):627–39.
26. Diaz-Soto MP, Garcia-Tsao G. Management of varices and variceal hemorrhage in liver cirrhosis: a recent update. THER ADV GASTROENTER. [Journal Article; Review]. 2022 2022-1-20;15:1098284688.
27. Wan S, Wei Y, Zhang X, Yang C, Song B. CT-derived quantitative liver volumetric parameters for prediction of severe esophageal varices and the risk of first variceal hemorrhage. EUR J RADIOL [Journal Article]. 2021 2021-11-1;144:109984.
28. Fu S, Chen D, Zhang Z, Shen R. Predictive value of spectral computed tomography parameters in esophageal variceal rupture and bleeding in cirrhosis. TURK J GASTROENTEROL [Journal Article]. 2023 2023-4-1;34(4):339–45.
29. Wang J, Zhang L, Cheng SM, Li B, Shen J. The evaluation of portal hypertension in cirrhotic patients with spectral computed tomography. ACTA RADIOL [Journal Article]. 2023 2023-3-1;64(3):918–25.
30. Gaduputi V, Patel H, Sakam S, Neshangi S, Ahmed R, Lombino M et al. Value of portal venous system radiological indices in predicting esophageal varices. CLIN EXP GASTROENTER. [Journal Article]. 2015 2015-1-20;8:89–93.
31. Lee CM, Lee SS, Choi WM, Kim KM, Sung YS, Lee S et al. An index based on deep learning-measured spleen volume on CT for the assessment of high-risk varix in B-viral compensated cirrhosis. EUR RADIOL. [Journal Article]. 2021 2021-5-1;31(5):3355–65.
32. Tani T, Sato K, Sakamoto K, Ito E, Nishiyama M, Urakawa H et al. Importance of extracellular volume fraction of the spleen as a predictive biomarker for high-risk esophago-gastric varices in patients with chronic liver diseases: A preliminary report. EUR J RADIOL [Journal Article]. 2021 2021-10-1;143:109924.

Publisher's note